Journal of Building Engineering ∎ (∎∎∎∎) ∎∎∎–∎∎∎

Contents lists available at ScienceDirect

Journal of Building Engineering

journal homepage: www.elsevier.com/locate/jobe

On the applicability and accuracy of fire design methods for open cold-formed steel beams

Luís Laím, João Paulo C. Rodrigues *

ISISE - Institute for Sustainability and Innovation in Structural Engineering, University of Coimbra, Portugal

ARTICLE INFO

Article history:
Received 26 January 2016
Received in revised form
12 September 2016
Accepted 13 September 2016

Keywords:
Fire
Cold-formed steel
Beam
Restrained thermal elongation
Design
Experimental
Numerical

ABSTRACT

This paper presents the results of an experimental and numerical investigation on the structural behaviour of cold-formed steel C and lipped-I beams subjected to uniform temperature distributions under standard fire conditions. A total of 18 specimens divided into four-point bending tests under fire conditions and under 3 different restraining conditions (including no restraints, partial axial restraint to the thermal elongation of the beam and both partial axial and rotational restraints at the beam supports) have been conducted. Local buckling, distortional buckling, lateral-torsional buckling and their interactions were observed in the tests. Then, the tests were modelled by the finite element programme Abaqus and, at the end, the numerical results showed good agreement with the experimental results in terms of axial restraining forces, vertical displacements, critical temperatures and buckling modes. The simulated results were still compared with the predictions from the currently European design rules (EN 1993-1.2:2005), in order to observe if there are safe and consistent regulations for fire design of these members. Finally, the numerical simulations have mainly shown that these design methods for CFS beams may be quite unsafe or over-conservative depending strongly on their boundary conditions.

1. Introduction

Cold-formed steel (CFS) members under high levels of compression may easily exhibit local (wall transverse bending only), distortional (both wall transverse bending and cross-section distortion) and global (lateral-torsional) buckling [1–4]. Local buckling is particularly prevalent and is characterised by the relatively short wavelength buckling of individual plate elements. Distortional buckling involves both translation and rotation at the compression flange/lip fold line of the member [5]. These special buckling modes are the most interesting and complex subjects within this research field. Beyond them, interactive buckling modes between or among the above ones are the most frequently in the CFS flexural members. This is why, the strength calculations of cold-formed steel members are carried out at several levels of complexity depending on the purpose of its use. For the standardised design of flexural members at ambient temperature the Effective Width Method (EWM) and the recently developed Direct Strength Method (DSM) [6] may be applied. The EWM is formally available in the EN 1993-1.3:2004 [7], EN 1993-1.5:2006 [8] and in the AISI S100-1996 [9], whereas the DSM is available in the Appendix 1 of the North American Specification [10] and the Australia/ New Zealand Standard [11]. The EWM, introduced by Von Kármán et al. in 1932 [12], performs a reduction of the plates that comprise a cross-section based on the stability of the individual plates for the prediction of the local buckling strength. It is noticed that this method is a semi-empirical calibrated formulation which takes into account the local buckling effects for thin-walled sections, but does not have sufficient procedures for predicting the distortional buckling failure. However, the EN 1993-1.3:2004 [7] provides specific provisions for the distortional buckling strength of CFS flexural members. This method adopted in the Eurocode considers the distortional buckling by using a reduced thickness in the calculation of the effective area of the edge stiffener and the distorted part of the compression flange. The reduction factor of thickness for distortional buckling depends among other parameters on the elastic buckling stress of the edge stiffener and the material yield strength. On the other hand, the DSM was initially proposed by Schafer and Peköz in 1998 [13] and it is based on the member elastic stability in contrast to the EWM. The essential difference between these two methods is therefore the replacement of plate stability by member stability. First, all elastic instability loads (or moments) for the gross cross-section should be determined (local, distortional and global buckling mode) as well as the load (or moment) that causes the section to yield. Then the member strength can be directly determined by predicting the load (or moment) capacities separately for global,

* Correspondence to: Departamento de Engenharia Civil, Faculdade de Ciências e Tecnologia da Universidade de Coimbra, Rua Luís Reis Santos, Pólo II da Universidade, 3030-788 Coimbra, Portugal.
E-mail address: jpaulocr@dec.uc.pt (J.P.C. Rodrigues).

http://dx.doi.org/10.1016/j.jobe.2016.09.004
2352-7102/

Nomenclature

CFS	cold-formed steel
DSM	direct strength method
EWM	effective width method
FEA	finite element analysis
E	modulus of elasticity of steel
L	beam span
$M_{b,Rd}$	design value of the resistant buckling moment
$M_{b,\ fi,t,\ Rd}$	design lateral-torsional buckling resistance moment at time t of a laterally unrestrained beam in fire situation
$M_{fi,\theta,\ Rd}$	design moment resistance of the cross-section at temperature θ
M_{cr}	elastic critical moment for lateral–torsional buckling
M_y	appropriate bending moment
P_0	initial applied load on the beam
W_{eff}	effective section modulus of the cross-section
W_y	appropriate section modulus of the cross-section
f_y	yield strength of steel
h	height of the cross-section
$k_{E,\theta}$	reduction factor for the modulus of elasticity of steel at temperature θ
k_a	axial restraint to the thermal elongation of the beam
$k_{a,b}$	axial stiffness of the beam
k_r	rotational stiffness of the beam supports about the major axis
$k_{r,b}$	rotational stiffness of the beam about the major axis
$ky_{,\theta}$	reduction factor for the yield strength of steel at temperature θ
t	thickness of the cross-section
$\gamma_{M,\ fi}$	partial material safety factor in fire design
θ_{cr}	critical temperature of the beam
$\bar{\lambda}_{LT}$	non-dimensional slenderness for lateral-torsional buckling at ambient temperature
$\bar{\lambda}_{LT,\theta}$	non-dimensional slenderness for lateral-torsional buckling at temperature θ
$\chi_{LT,\ fi}$	reduction factor for lateral-torsional buckling in the fire design situation

local and distortional buckling, in the same way of EN 1993-1.1:2004 [14] predicts the design buckling resistance of a hot-rolled steel member, in other words, basing on reduction factors for the corresponding buckling curves and taking also into account the post-buckling reserve and the interaction between these modes.

When it comes to fire, the design rules are commonly based on past research on hot-rolled steel members. Note that due to the high slenderness of the cross-section's walls (high ratio width/thickness of the wall), CFS sections are mostly found in class 4 cross-sections, in contrast to hot-rolled steel sections which are mostly class 1 or 2. However, the simplified design methods presented in the EN 1993-1.2:2005 [15] can be used for CFS members according to its Annex E, but the area of the member cross-section must be replaced by the effective area and the section modulus by the effective section modulus, determined in accordance with EN 1993-1.3:2004 [7] and EN 1993-1.5:2006 [8], i.e. based on the material properties at 20 °C. Besides, the design yield strength of steel should be taken as the 0.2% proof strength. To further exacerbate the situation, EN 1993-1.2:2005 [15] still recommends a limit of 350 °C for the maximum temperature of members with class 4 cross-sections, which seems to be overly conservative [16–18]. Therefore, it is the objective of this research to investigate the accuracy of the current design guidelines for open CFS flexural members subjected to uniform temperature distributions under standard fire conditions. To accomplish this goal, a series of experimental tests and numerical simulations were performed at Coimbra University (UC) in Portugal on CFS beams with different open cross-sections (C and lipped-I sections) and boundary conditions (different levels of axial and rotational restraints at beam supports). These results were thereby compared with the predictions from the currently European design rules (EN 1993-1.2:2005 [15]), in order to observe if there are safe and consistent regulations for fire design of these members and for providing economical CFS structures in case of fire. Still note that, in the near future, these studies will be the basis of an analytical study for the development of simplified calculation methods for fire design of axially and rotationally restrained CFS beams.

2. Experimental and numerical models

2.1. Testing details

The experimental tests on CFS beams subjected to uniform temperature distributions under standard fire conditions were conducted at the Laboratory of Testing Materials and Structures (LEME) of Coimbra University (UC), in Portugal. The experimental programme consisted of 18 experimental tests on CFS beams, composed of just one (C beam) and two (2C beams) profiles. Six of which were just simply supported beams (Fig. 2a), 6 others were the same beams but with restrained thermal elongation (Fig. 2b), and the others were beams with axial and rotational restraint (Fig. 2c). All these profiles had the same nominal thickness (2.5 mm), nominal flange width (43 mm) and inside bend radius (2 mm). The edge stiffeners had 15 mm long and the nominal web

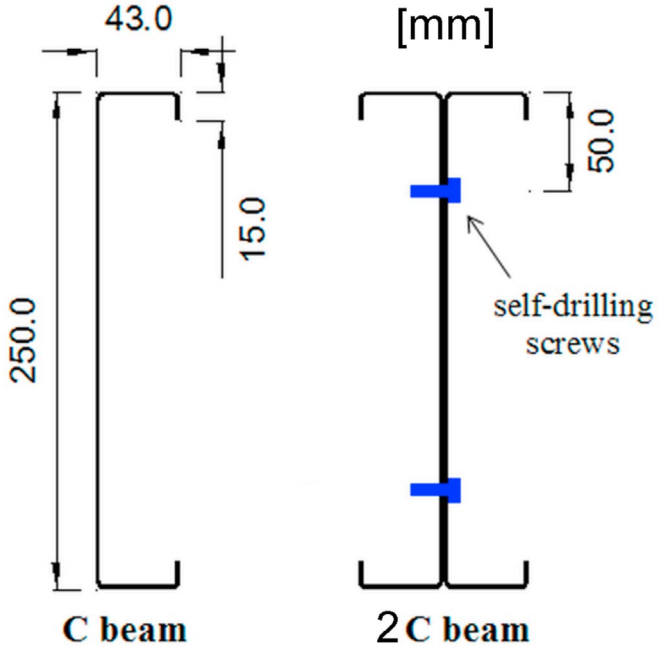

Fig. 1. Scheme of the cross-sections of the tested beams.

Please cite this article as: L. Laím, J.P.C. Rodrigues, On the applicability and accuracy of fire design methods for open cold-formed steel beams, Journal of Building Engineering (2016), http://dx.doi.org/10.1016/j.jobe.2016.09.004

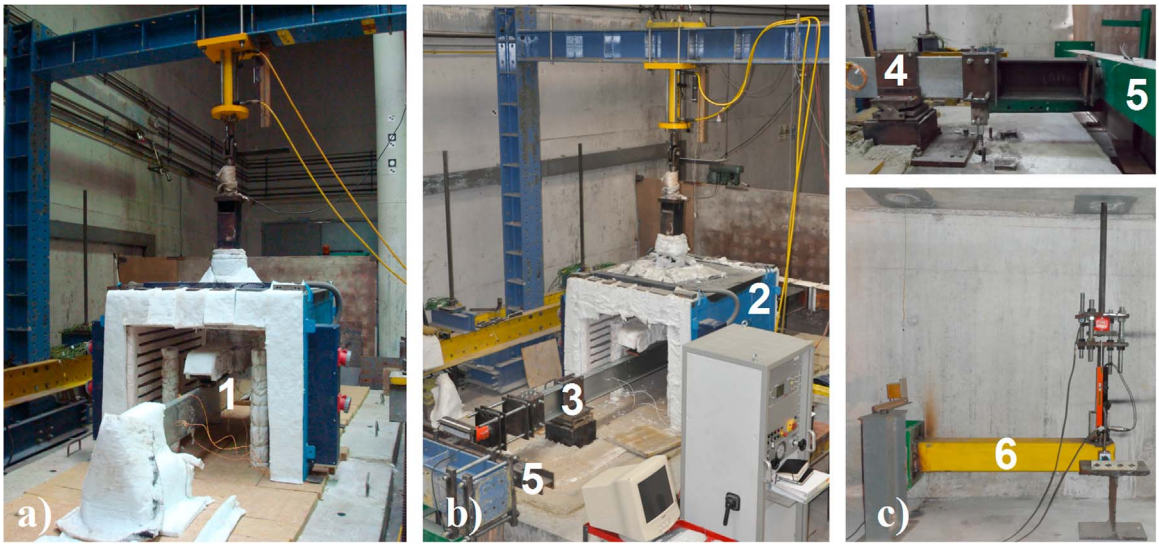

Fig. 2. Overview of the experimental set-up for flexural tests of simply supported (a), axially restrained (b) and both axially and rotationally restrained (c) CFS beams: 1 - specimen; 2- horizontal furnace; 3 - roller support; 4 - pinned support; 5 - axial restraining beam; 6 - rotational restraining beam.

Table 1
Experimental test plan.

Test reference	$\bar{\lambda}_{LT}$	$M_{b,Rd}$ (kN m)	$k_{a,b}$ (kN/mm)	$k_{r,b}$ (kN m/rad)	P_0 (kN)	k_a (kN/mm)	k_r (kN m/rad)
B-C	1.61	3.93	61	1984	3.93	0	0
B-I	1.22	11.88	124	4018	11.88	0	0
B_ka-C	1.61	3.93	61	1984	3.93	15	0
B_ka-I	1.22	11.88	124	4018	11.88	15	0
B_ka+kr-C	1.61	3.93	61	1984	3.93	15	150
B_ka+kr-I	1.22	11.88	124	4018	11.88	15	150

width had 250 mm (Fig. 1). As it can also be seen in this figure, the lipped I beams (2C beams) consisted of two C connected by the respective profiles' web. These connections were materialised by means of 6.3 mm diameter steel self-drilling screws. The beam span, L, was 3.0 m for all specimens and the distance between the screws along beam was about 1 m (L/3). All profiles were still made of S280GD+Z structural steel and the screws of S235 steel. These profiles were manufactured by the company PERFISA S.A., which is specialised in the fabrication of CFS profiles, and the choice of the cross-sections and the distance between the screws was based on the observation of CFS structures and design projects for this kind of buildings, representing commonly used details in several countries. This experimental programme is also summarised in Table 1. Note that, the reference B_ka+kr-C_3 indicates the third test (3) of the C (C) beam (B) with axial (*ka*) and rotational (*kr*) restraint.

The test set-up essentially consisted of a reaction frame, a hydraulic jack to apply loading, a modular electric fire resistance furnace to simulate fire conditions, and roller and pinned supports to provide a simply supported beam, as illustrated in Fig. 2. The beams were loaded at two points 1.0 m (one-third of the beam span) from the supports of the beam in such a way that between the two loading points the beam was under pure bending state (four-point bending test). This load was 50% of the design value of the load-bearing capacity of the beams at ambient temperature and calculated in accordance with the methods proposed in Eurocode 3 [7,8,14] and calculated for simply-supported boundary conditions, as it is common observed in design projects for this kind of structures. The specimens (1) were then heated with a horizontal modular electric furnace (2) and according to a fire curve as near as possible to the standard fire curve ISO 834 [19]. During the heating period, the load was kept constant until the specimen buckled. This furnace was 4500 mm long, 1000 mm wide and 1000 mm tall in internal dimensions and capable to heat up to 1200 °C and to follow fire curves with different heating rates. These beams were supported by a roller (3) and pinned (4) support, which were made of refractory stainless steel, typically used for elevated temperature applications. Furthermore, the experimental system still comprised four restraining steel beams, two of them (5) to simulate the axial restraint to the thermal elongation of the beam and the other two (6) with the purpose of simulating the rotational stiffness of the beam supports. Hence, the axial restraining system was composed of two simply supported beams (5) and the rotational restraining system of two cantilever beams (6), as it can be seen in Fig. 2. It is noticed that these last two beams were placed in the basement floor of the Laboratory, below the testing floor. Also note that the specimen was connected to the rotational restraining beams by means of pin-ended steel threaded rods (they passed through the holes of the slab of the Laboratory) (Fig. 2c). In addition, there was still a threaded rod system (near the roller support) (Fig. 2b) with the purpose of eliminating the clearances between the specimen and the axial restraining beams. A steel semi-sphere was also placed between the ends of the specimen and those beams so that this kind of test set-up allowed studying separately the effects of axial and rotational restraining to thermal elongation on the fire resistance of CFS beams. Lastly, load cells were mounted in order to monitor the axial restraining forces generated in the test specimen and the restraining forces due to the rotational restraint imposed by cantilever beams (6) during the fire tests. Further detailed information or clarification regarding the experimental research can be easily found in the study of Laím *et al.* (2014) [20].

Please cite this article as: L. Laím, J.P.C. Rodrigues, On the applicability and accuracy of fire design methods for open cold-formed steel beams, Journal of Building Engineering (2016), http://dx.doi.org/10.1016/j.jobe.2016.09.004

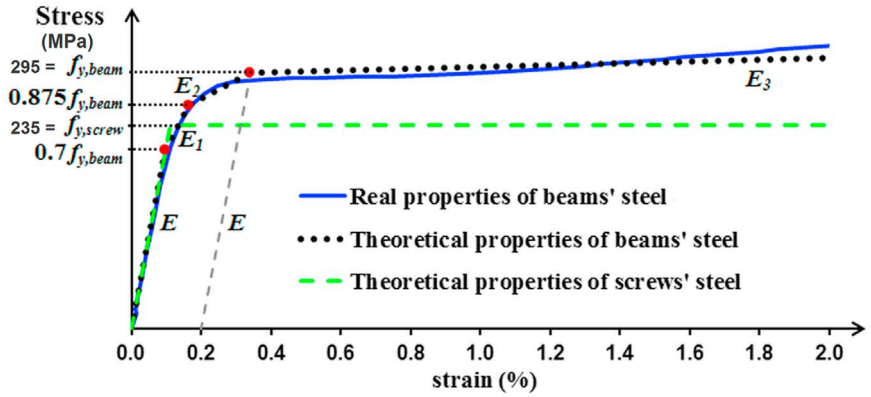

Fig. 3. Stress-strain relationship of the beam's and screw's steel.

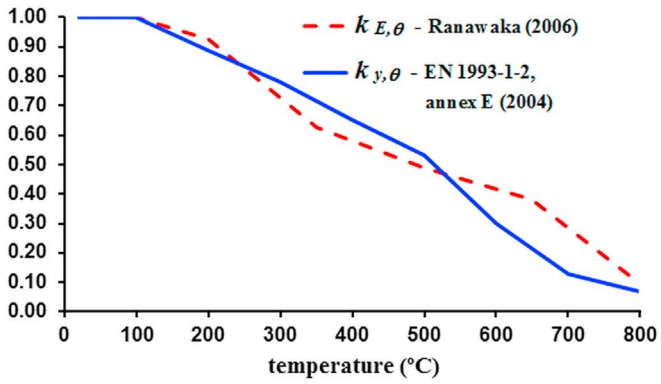

Fig. 4. Reduction factors for the stress-strain relationship of CFS sections at elevated temperatures.

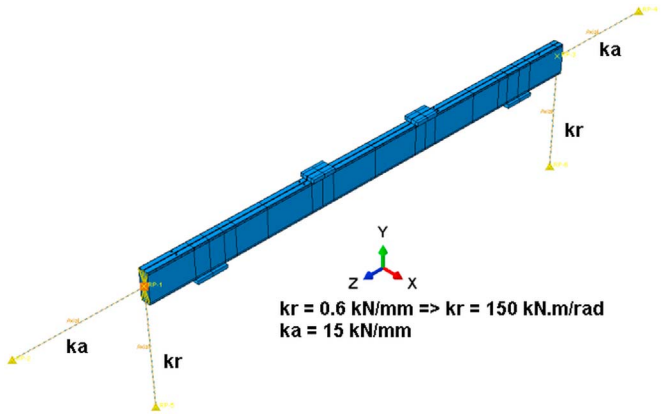

Fig. 5. Numerical model used in the finite element analysis.

2.2. Finite element modelling

2.2.1. Basic parameters

For the simulation of CFS beams and the analysis of their fire behaviour, the finite element programme ABAQUS [21] was used. Therefore, all CFS beams were modelled by using shell elements (S4R) for the profiles and solid elements (C3D8R) for the screws [22,23] and a suitable finite element mesh of 10×10 mm was generated automatically by Abaqus software and used in all simulations. The stress-strain relationship of CFS profiles was assumed the same across all cross-section and described by a gradual yielding behaviour followed by a considerable period of strain hardening, whereas an elastic-perfectly plastic behaviour was assumed for the steel screws. Fig. 3 shows the stress-strain curve used in the finite element analysis (FEA) for the CFS profiles based on tensile coupon test results and at the same time on other studies of literature [24,25]. So, it was tried to reproduce as faithful as possible the stress-strain relationship of the steel coupon specimens taken from the web of the tested beams in the longitudinal direction. A yield strength of 295 MPa, a tensile strength of 412 MPa and a modulus of elasticity of 208 GPa were obtained from those tests at ambient temperature. The initial slope of the theoretical stress-strain curve was taken as the elastic modulus, E, of the material. The second, third and fourth slope (E_1, E_2 and E_3) of the curve were defined by tangent modulus which were respectively 38%, 10% and 0.5% of the elastic modulus. Therefore, a gradual yielding behaviour was idealised by using a bilinear representation with tangent modulus E_1 and E_2 between 70% and 100% of the yield strength, f_y, with an intermediate point at a stress of 0.875 f_y [25]. All other components were modelled as elastic, i.e. the elastic modulus was equal to 210 GPa and the Poisson's ratio to 0.3. On the other hand, the thermal properties of the CFS at elevated temperatures considered in the model (mass density, thermal conductivity and specific heat) were those given in EN 1993-1.2:2005 [15]. The reduction factors for the yield strength of steel at elevated temperatures were still obtained from the EN1993-1.2:2005, annex E [15], whereas the reduction factors for the modulus of elasticity were taken from the experimental data of Ranawaka (2006) [26] (Fig. 4). The reason for the choice of these parameters was due to the fact that these members are mostly class 4 cross-sections and their manufacturing process is different from the hot-rolled steel members and, as it can be seen further ahead on this paper, these parameters still allowed to well estimate the structural behaviour of these beams. Moreover, these reduction factors fit well with the experimental values obtained from tensile coupon tests at elevated temperatures previously carried out by the authors [27].

A three-dimensional numerical model was employed to describe all buckling modes observed in the four-point bending tests at high temperatures (Fig. 5). As it can be seen in this figure, the axis system of the model is such that Z axis lies in the longitudinal direction of the beam while X and Y axes lie in the major and minor axes of the beam's cross-section, respectively. The beam supports and the loading were applied on rigid plates attached to beams so as to distribute possible concentrated forces on them. All simulated beams were still modelled using the centre line dimensions and, whereas a tangential friction coefficient of 0.2 and a hard contact between the profile surfaces was assumed, a rough and hard contact between the profiles and the screws was considered. Lastly, for the modelling of the axial, *ka*, and rotational, *kr*, restraining system, a linear spring model was used (Fig. 5), in the same way the four restraining steel beams were used in the real experimental set-up. Abaqus allows the user to define axial spring elements connected to a node of the member and a support that

Please cite this article as: L. Laím, J.P.C. Rodrigues, On the applicability and accuracy of fire design methods for open cold-formed steel beams, Journal of Building Engineering (2016), http://dx.doi.org/10.1016/j.jobe.2016.09.004

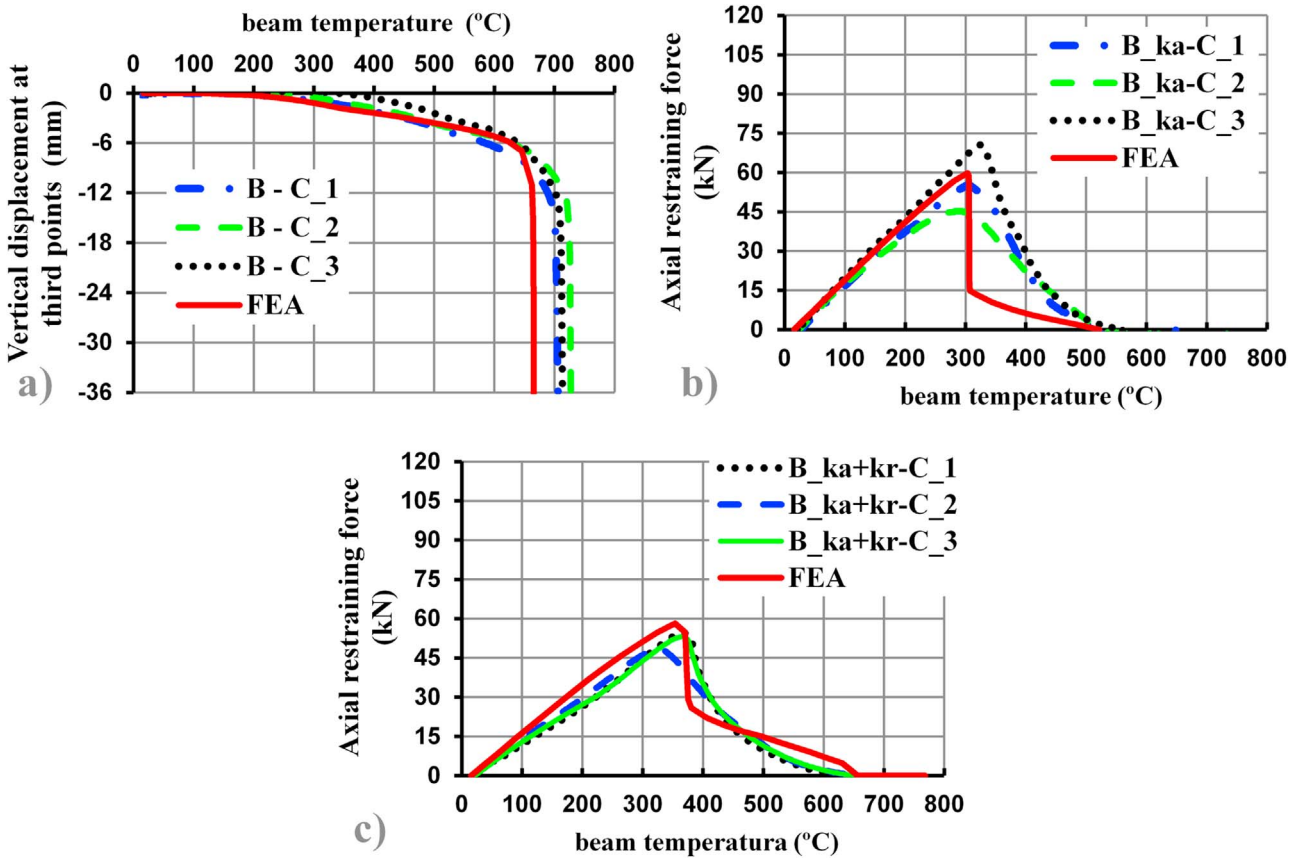

Fig. 6. Comparison of the FEA and experimental results for the simply supported C beams (a), axially restrained C beams (b) and both axially and rotationally restrained C beams (c).

have the appropriate stiffness coefficients. The springs were connected to the beams at the centre of the cross-section by means of the *Coupling Constraints option in Abaqus [21]. The kinematic coupling constraint was employed in order to constrain the motion of the end surfaces of the beams to the motion of a single point, in this case the centre point of the beam's cross-section.

2.2.2. Analysis procedure

Three types of analysis were separately employed by using the developed finite element model: elastic buckling, heat transfer and nonlinear static analyses. Elastic buckling analysis was performed to establish the buckling modes which were observed in the experimental tests, thus using them to input the geometric imperfections in the nonlinear analysis. After knowing their effects on structural response of this kind of beams and comparing with the results of the experimental tests, it was observed that a suitable maximum value for global imperfections was found to be approximately L/1000, for distortional imperfections t and for local imperfections h/200, where L, t and h stand for the length of the beams, the thickness and the height of the beam's cross-section, respectively.

In the heat transfer analysis, a 4-node linear heat transfer quadrilateral (DC2D4) was still chosen to estimate the temperature distribution in the cross-sections of the beams. The fire action was defined by two types of surface, namely, "film condition" and "radiation to ambient" which correspond respectively to heat transfer by convection and radiation. As it is recommended by the EN 1991-1.2:2002 [28], a coefficient of heat transfer by convection equal to 25 W/(m^{2}K) was used and the resultant emissivity was taken as 0.2 (considering the emissivity of the furnace's electric resistance and the profiles equal to 0.7 and 0.3, respectively), due to the mirror surface of the zinc coating on the profiles used [29]. Note that the thermal analysis (model) was only used in the parametric analysis and not in the calibration of the structural model since in this case the experimentally measured temperatures were used as input data. Finally, a structural analysis was undertaken (using the Abaqus/Standard direct solver) with the purpose of simulating the performance of the CFS beams under fire conditions until failure. The nonlinear geometric parameter (*NLGEOM=ON) was set to deal with the geometric nonlinear analysis, namely, with the large displacement analysis. Also note that before the heating stage, a serviceability load was applied on the beams. This load level was a percentage (30, 50 or 70%) of the design value of the load-bearing capacity of the beams at ambient temperature, calculated in accordance with the methods proposed in EN 1993-1.1:2004 [14], EN 1993-1.3:2004 [7] and EN 1993-1.5:2006 [8] and calculated for simply-supported boundary conditions, as it is common observed in design projects for this kind of structures. During the heating phase, the load was kept constant until the specimen buckled, where the beam deformation was too large, $L^2/(400\,h)$ (failure criteria in terms of deformation [19]), which corresponded approximately to the time when the beams no longer had any loadbearing capacity against the axial restraining forces (failure criteria in terms of strength), i.e., when the compression force in beams was totally released, as it can be seen in [20]. Hence, the critical (failure) temperature of the beams was defined as the one which corresponded to that time.

3. Accuracy of the finite element model

3.1. Comparison between the experimental and finite element

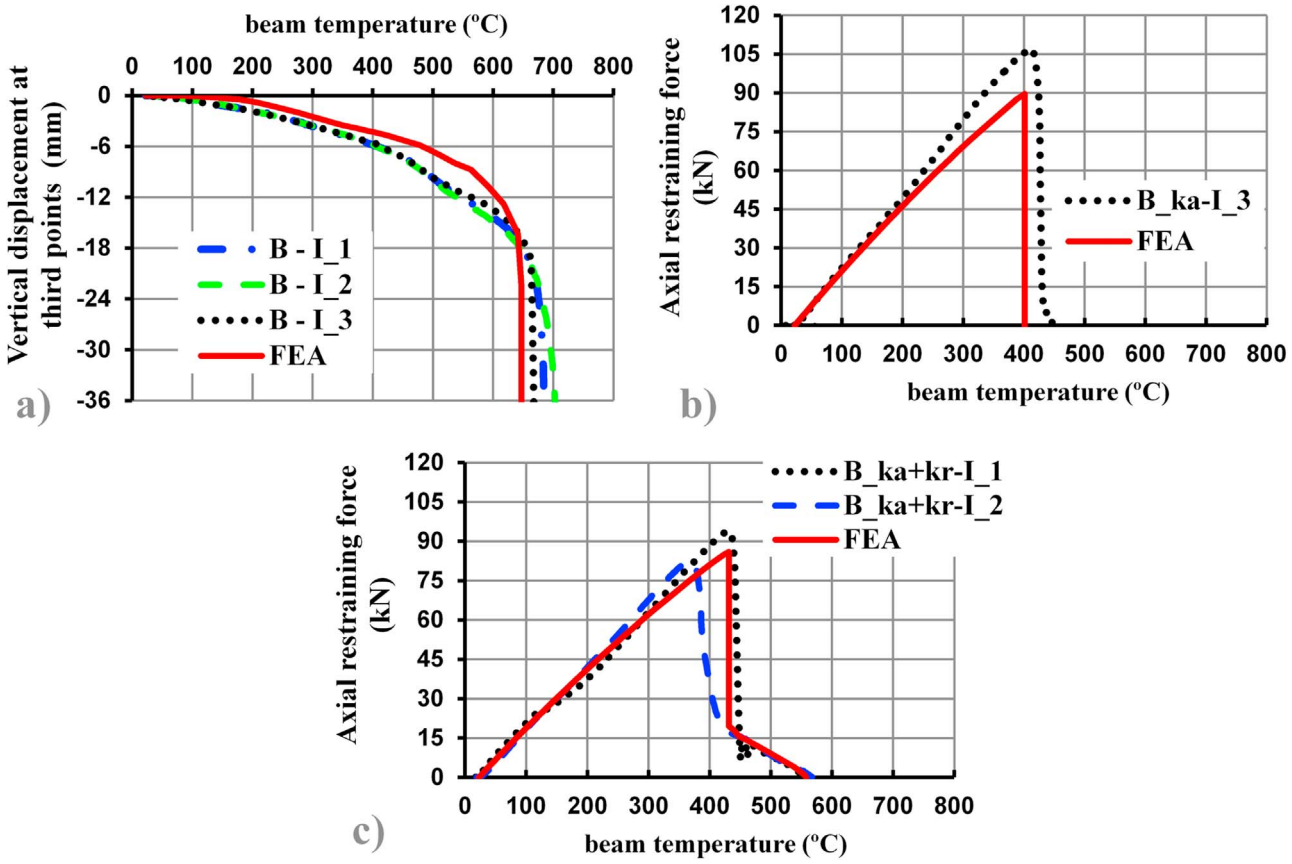

Fig. 7. Comparison of the FEA and experimental results for the simply supported lipped I beams (a), axially restrained lipped I beams (b) and both axially and rotationally restrained lipped I beams (c).

Table 2
Experimental and FEA critical temperatures.

Test reference	θ_{cr} (°C)		Comparison (%)
	Test	FEA	
B-C	718	666	−7.3
B-I	691	647	−6.4
B_ka-C	529	522	−1.4
B_ka-I	544	504	−7.3
B_ka+kr-C	641	656	2.4
B_ka+kr-I	567	558	−1.7

analysis results

To check the accuracy of the Abaqus model, all the tests have been simulated. Below comparisons of the experimental and numerical results are given to demonstrate the authors' confidence in using Abaqus to model the fire resistance and behaviour of these beams outside the bounds of the original experimental tests. Therefore, Figs. 6 and 7 show a general idea of how the C and lipped-I beams with different boundary conditions (simply supported (Figs. 6a and 7a), axially restrained (Figs. 6b and 7b) and both axially and rotationally restrained (Figs. 6c and 7c)) might behave as a function of its temperature and in terms of vertical deformation (Figs. 6a and 7a) or axial restraining forces (Figs. 6b,c, 7b and c), under fire conditions. It can be seen from these results, that in general the axial restraint had a negative effect on the critical temperature of the beams in contrast to the rotational restraint, as it was expected. It is noticed that when 15kN/mm of axial restraint was imposed on the C beams, their critical temperature decreased about 25% (from 718 to 529 °C), but when it was also introduced 150kN.m/rad of rotational restraint to the beam supports, the critical temperature of these beams increased about 20% in relation to axially restrained C beams (from 529 to 641 °C). Finally, all curves from finite element analysis (FEA) fit closely with the experimental curves and, as well as that, the numerical critical temperatures were in very good agreement with the experimental ones (Table 2). In fact, in the most cases, the critical temperatures assessed by the numerical model were 10% lower than the experimentally measured results, indicating that the estimated data were on the safe side but not too conservative either.

3.2. Comparison between the experimental and FEA failure modes of the beams

For instance, Fig. 8 illustrates the FEA failure modes of the simply supported (Fig. 8b) and both axially and rotationally restrained C beams (Fig. 8d) under fire conditions, which can be respectively contrasted to the experimental failure modes as shown in Fig. 8a and c. Once again, it can be seen clearly by both kinds of figures that the developed finite element model predicted the behaviour of CFS beams with an acceptable precision. The failure modes of the beams involved distortional, lateral-torsional buckling and still, but less visible, local buckling. It was possible to observe that the lateral-torsional buckling was the main failure mode responsible for the collapse of the simply supported C and lipped-I beams (Fig. 8a and b), whereas shear buckling (extensive diagonal web buckling between the beam supports and the loading points) was the mode responsible for the collapse of the respective axially and rotationally restrained beams (Fig. 8c and d). The final configuration of the axially restrained beams was not

Please cite this article as: L. Laím, J.P.C. Rodrigues, On the applicability and accuracy of fire design methods for open cold-formed steel beams, Journal of Building Engineering (2016), http://dx.doi.org/10.1016/j.jobe.2016.09.004

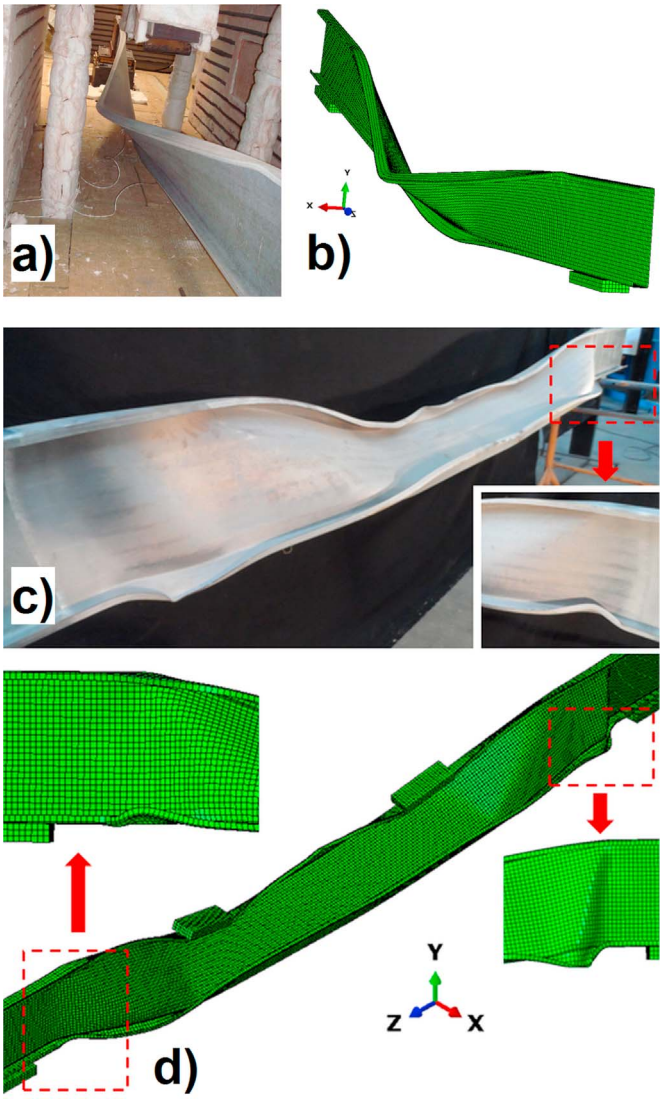

Fig. 8. Experimental (a and c) and numerical (b and d) configuration of the deformed C beam with no restraints (a and b) and with axial and rotational restraint (c and d) after fire test.

presented here because their failure modes were similar to the simply supported beams.

4. Accuracy of European fire design rules

At present, design calculation methods for cold-formed thin-walled members in fire are not as well developed as for hot-rolled members. Note that the design rules given in EN 1993-1.2:2005 [15] for hot-rolled steel are applicable for cold-formed steel members within the scope of EN 1993-1.3:2004 [7]. In other words, EN 1993-1.2:2005 [15] recommends that the effective properties of a steel plate should be kept unchanged as at ambient temperature, the design yield strength of steel should be taken as the 0.2% proof strength and the buckling curve should be the same as that for hot-rolled steel members. Therefore, the design lateral-torsional buckling resistance moment of a laterally unrestrained beam is given by,

$$M_{b,fi,t,Rd} = \chi_{LT,fi}\frac{M_{fi,\theta,Rd}}{\gamma_{M,fi}} = \chi_{LT,fi}\bullet W_y \bullet k_{y,\theta}\bullet\frac{f_y}{\gamma_{M,fi}} \tag{1}$$

W_y is the appropriate section modulus of the compression flange depending on the class of cross section (plastic, elastic or effective section modulus). For cold-formed steel members, W_y should be taken as the effective section modulus (W_{eff}) according to EN 1993-1.3:2004 [7]. f_y is the 0.2% yield strength of steel. $\gamma_{M,\,fi}$ is the partial factor for the respective material property for fire situation. $\chi_{LT,\,fi}$ is defined as follows (EN 1993-1.2:2005 [15]),

$$\chi_{LT,fi} = 1/\left(\Phi_{LT,\theta} + \sqrt{\Phi^2_{LT,\theta} - \bar{\lambda}^2_{LT,\theta}}\right) \tag{2}$$

with

$$\Phi_{LT,\theta}=0.5\left[1+\alpha\bullet\bar{\lambda}_{LT,\theta} + \bar{\lambda}^2_{LT,\theta}\right] \tag{3}$$

$$\alpha=0.65\sqrt{235/f_y} \tag{4}$$

$$\bar{\lambda}_{LT,\theta} = \bar{\lambda}_{LT}\sqrt{k_{y,\theta}/k_{E,\theta}} \tag{5}$$

$$\bar{\lambda}_{LT} = \sqrt{\frac{M_y}{M_{cr}}} = \sqrt{\frac{W_{eff}f_y}{M_{cr}}} \tag{6}$$

$\bar{\lambda}_{LT}$ is non-dimensional slenderness of the beam at ambient temperature. M_{cr} is the elastic critical moment of the gross cross section for lateral-torsional buckling about the strong axis. $k_{y,\theta}$ and $k_{E,\theta}$ are the reduction factors for the 0.2% yield strength and the modulus of elasticity of steel at the maximum temperature in the compression flange θ reached at time t, respectively. Fig. 9 displays the comparison of the FEA results obtained for different lengths of C and lipped-I beams under simply supported boundary conditions and fire with the beam design curve obtained from the fire

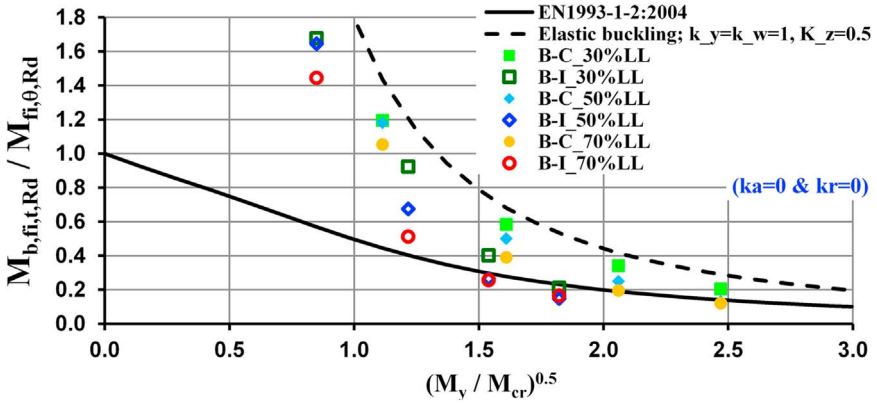

Fig. 9. Comparison of FEA results with EN 1993-1.2:2005 [15] for simply supported C and lipped I beams.

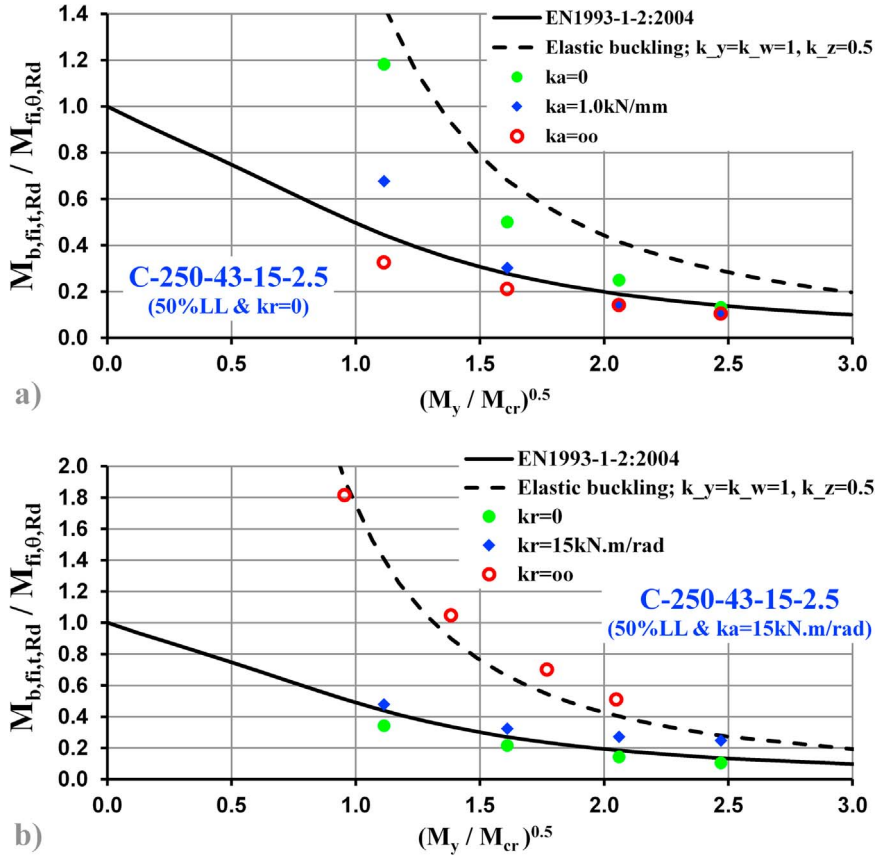

Fig. 10. Comparison of FEA results with EN 1993-1.2:2005 [15] for axially restrained C beams (a) and axially and rotationally restrained C beams (b).

design code, EN 1993-1-2:2005 [15]. Despite all FEA results are lower than the respective elastic lateral-torsional buckling results, it can be seen that code predictions may be over-conservative for slenderness values lower than 1.3 ($(M_y/M_{cr})^{0.5} < 1.3$). Note that, the effective buckling length factors about the major (k_y) and minor (k_z) axis of the beam were respectively assumed to be equal to 1.0 and 0.5 and the factor which accounts for the beam end warping (k_w) equal to 1.0. The higher the non-dimensional slenderness, the higher the accuracy of the predicted buckling moment capacity was. However, it is interesting to point out that EN 1993-1-2:2005 predictions [15] for beams with 70% of load level (*70%LL*) appear to be unsafe, even for some lipped-I beams with 50% of load level ($1.5 < (M_y/M_{cr})0.5 < 2.0$). Lastly, when axial restraint, k_a, was imposed on beams, it was observed that the code predictions may be very unsafe (Fig. 10a) and when rotational restraint is also introduced at beam supports the predictions may be too conservative (Fig. 10b).

5. Conclusions

This paper has described a finite element model developed to simulate the fire resistance and behaviour of cold-formed steel C and lipped-I beams under flexural conditions and 3 different restraining conditions (including no restraints, partial axial restraint to the thermal elongation of the beam and both partial axial restraint and partial rotational restraint at beam supports). It was first observed that the model was found to be accurate in predicting the structural behaviour of such beams in fire situation, especially their critical temperatures, with an average difference of not more than 4% when compared with the results obtained from several experimental tests previously performed in Laboratory by the authors [20]. Despite this, the main conclusion of this investigation was that the design rules given in EN 1993-1-2:2005 [15] may not be suitable for designing cold-formed steel flexural members subjected lateral-torsional buckling. It seems that its design methods give too conservative results both for low initial applied loads on the beams and for low slenderness values, while for high slenderness and high initial load levels they appear to be unsafe. On the other hand, these design guidelines did not say anything concerning the fire design of flexural members under different types of restraining conditions (axial and / or rotational restraint), which may also result in overly conservative or quite unsafe design methods. Hence, new simplified calculation methods for fire design of CFS members should emerge. To ensure fire safety of structures, CFS members should be properly designed so that they can withstand unexpected fire situations. Engineers and architects face problems in using cold-formed steel members in structures because of lack of suitable design specifications for fire conditions. This is why there is an urgent and absolute need of finding new fire design methods for CFS members and this research work may be one of the first steps in the right way for solving this problem/need.

Acknowledgements

The authors gratefully acknowledge to the Portuguese Foundation for Science and Technology – FCT (www.fct.mctes.pt) for its support under the framework of research project PTDC/ECM/116859/2010 and for the postdoctoral scholarship SFRH/BPD/94037/2013 given to the first author, as well as to the Human Potential Operational Programme (POPH), the European Social Fund and the National Strategic Reference Framework (QREN). The

authors would also like to thank the Portuguese cold-formed steel profile maker PERFISA S.A. (www.perfisa.net) for their support.

References

[1] N.D. Kankanamge, M. Mahendran, Behaviour and design of cold-formed steel beams subject to lateral–torsional buckling, Thin-Walled Struct. 51 (2012) 25–38.

[2] N.D. Kankanamge, M. Mahendran, Behaviour and design of cold-formed steel beams subject to lateral–torsional buckling at elevated temperatures, Thin-Walled Struct. 61 (2012) 213–228.

[3] S.-s Cheng, B. Kim, l-y Li, Lateral–torsional buckling of cold-formed channel sections subject to combined compression and bending, J. Constr. Steel Res. 80 (2013) 174–180.

[4] G.M. Bukasa, M. Dundu, Use of angle cleats to restrain cold-formed channels against lateral torsional instability, J. Constr. Steel Res. 123 (2016) 144–153.

[5] H. Wang, Y. Zhang, Experimental and numerical investigation on cold-formed steel C-section flexural members, J. Constr. Steel Res. 65 (2009) 1225–1235.

[6] B.W. Schafer, Review: the direct strength method of cold-formed steel member design, J. Constr. Steel Res. 64 (2008) 766–778.

[7] EN 1993-1.3: Eurocode 3: Design of steel structures - Part 1–3: Supplementary rules for cold-formed members and sheeting. European Committee for Standardization. Brussels, Belgium, 2004.

[8] EN 1993-1.5: Eurocode 3: Design of steel structures - Part 1–5: Plated structural elements, European Committee for Standardisation, Brussels, Belgium, 2006.

[9] AISI S100- 2007: North American Specification for the design of cold-formed steel structures members. American Iron and Steel Institute, Washington (DC), USA, 2007.

[10] AISI S100- 2004: Appendix 1: Design of cold-formed steel structural members using the Direct Strength Method. In: 2004 Supplement to the North American Specification for the Design of Cold-Formed Steel Structures. American Iron and Steel Institute, Washington (DC), USA, 2004.

[11] AS/NZS 4600(Cold formed steel structures, Australian/New Zealand Standard, 1996.

[12] T. Von Kármán, E.E. Sechler, L.H. Donnel, The strength of thin plates in compression, Trans. Am. Soc. Mech. Eng. 54 (1932) 53–57.

[13] B.W. Schafer, T. Peköz, Direct strength prediction of cold-formed steel members using numerical elastic buckling solutions, in: Proceedings of the 14th international specialty conference on cold-formed steel structures, St. Louis, Missouri, USA, 1998, pp. 69–76.

[14] EN 1993-1.1: Eurocode 3: Design of steel structures – Part 1.1 - General rules and rules for buildings. European Committee for Standardization. Brussels, Belgium, 2004.

[15] EN 1993-10.2: Eurocode 3: Design of steel structures – Part 1.2 - General rules-structural fire design. European Committee for Standardization, Brussels, Belgium, 2005.

[16] N.D. Kankanamge, Structural behaviour and design of cold-formed steel beams at elevated temperatures, pH.D. Thesis, Queensland University of Technology, Brisbane, Australia, 2010.

[17] W. Lu, P. Mäkeläinen, J. Outinen, Numerical simulation of catenary action in cold-formed steel sheeting in fire, J. Struct. Mech. 40 (3) (2007) 28–37.

[18] L. Laim, J.P.C. Rodrigues, L.S. Silva, Experimental analysis on cold-formed steel beams subjected to fire, Thin-Walled Struct. 74 (2014) 104–117.

[19] ISO 834-1: Fire resistance tests – elements of building construction, Part 1: General requirements, ISO - International Organization for Standardization, Switzerland, 1999.

[20] L. Laím, J.P.C. Rodrigues, L.S. Silva, Experimental analysis on cold-formed steel beams subjected to fire, Thin-Walled Struct. 74 (2014) 104–117.

[21] Abaqus/CAE Standard User's Manual, version 6.10-1, Simulia Corp., USA, 2010.

[22] P.B. Dinis, D. Camotim, Local/distortional mode interaction in cold-formed steel lipped channel beams, Thin-Walled Struct. 48 (2010) 771–785.

[23] C. Yu, B.W. Schafer, Simulation of cold-formed steel beams in local and distortional buckling with applications to the direct strength method, J. Constr. Steel Res. 63 (2007) 581–590.

[24] M. Feng, Y.C. Wang, J.M. Davies, Structural behaviour of cold-formed thin-walled short steel channel columns at elevated temperatures. Part 2: design calculations and numerical analysis, Thin-Walled Struct. 41 (2003) 571–594.

[25] L. Laím, J.P.C. Rodrigues, L.S. Silva, Experimental and numerical analysis on the structural behaviour of cold-formed steel beams, Thin-Walled Struct. 72 (2013) 1–13.

[26] T. Ranawaka, Distortional buckling behaviour of cold-formed steel compression members at elevated temperatures, pH.D. Thesis, Queensland University of Technology, Brisbane, Australia, 2006.

[27] H.D. Craveiro, J.P.C. Rodrigues, A. Santiago, L. Laím, Review of the high temperature mechanical and thermal properties of the steels used in cold formed steel structures – The case of the S280GD+Z steel, Thin-Walled Struct. 98 (2016) 154–168.

[28] (EN) 1991-1.2, Eurocode 1- Actions on structures - Part 1-2: General actions - Actions on structures exposed to fire. European Committee for Standardization, Brussels, Belgium, 2002.

[29] J. Jirků, F. Wald, the Temperature of Zinc coated Steel Members in Fire, in: Proceedings of the 8th International Conference on Structures in Fire 2014, Shanghai, China, pp. 129–136.

Please cite this article as: L. Laím, J.P.C. Rodrigues, On the applicability and accuracy of fire design methods for open cold-formed steel beams, Journal of Building Engineering (2016), http://dx.doi.org/10.1016/j.jobe.2016.09.004